




PERFORMANCE OF BRIDGES IN LATERALLY SPREADING GROUND UNDER LONG- VERSUS SHORT-DURATION GROUND MOTIONS

X. Wang⁽¹⁾ , Y. A. Heo⁽²⁾, A. Ye⁽³⁾, B. Ji⁽⁴⁾

⁽¹⁾ Postdoctoral Research Associate, Department of Civil Engineering, Hohai University, China, Email: x.wang@hhu.edu.cn

⁽²⁾ Assistant Professor, Department of Civil Engineering, Case Western Reserve University, USA, Email: yaheo@case.edu

⁽³⁾ Professor, State Key Lab of Disaster Reduction in Civil Engineering, Tongji University, China, Email: yeaijun@tongji.edu.cn

⁽⁴⁾ Professor, Department of Civil Engineering, Hohai University, China, Email: bhji@hhu.edu.cn

Abstract

This study characterizes the influence of long-duration ground motion on seismic demands and fragility performance of extended pile-shaft-supported bridges in liquefied and laterally spreading ground. To isolate the impact of amplitude and frequency content properties of ground motions, 91 pairs of spectrally equivalent long- and short-duration ground motion records are adopted in this study. An experimentally validated soil-pile-bridge coupled finite element model accounting for multiple sources of uncertainties in structural and geotechnical parameters is developed to perform a series of nonlinear dynamic analyses under the adopted long- and short-duration ground motions. Seismic demand parameters including soil lateral spreading displacement, peak bearing deformation, pile curvature, peak and residual column drifts are examined. Results indicate that long-duration ground motions do not bring detrimental effects to the estimates of peak bearing deformation; bridges designed under short-duration ground motions generally lead to conservative bearing deformation estimates under the spectrally equivalent long-duration counterparts. However, long-duration motions do bring detrimental effects to the estimates of pile curvature and column drifts by amplifying the demands as large as 2~6 times to short-duration motions. Such influence should be carefully considered in the seismic design of bridges.

Keywords: Bridge; Long-duration ground motion; Liquefaction; Lateral spreading; Seismic fragility



1. Introduction

Long-duration ground motions have been recorded in recent strong earthquakes such as the 2008 Wenchuan Earthquake and 2011 Tohoku Earthquake. A long-duration ground motion can be technically characterized by its significant duration (D_{s5-75} , the interval between 5% and 75% of the total Arias intensity [1]) greater than a threshold. Although consensus has not been reached, a threshold of 25 s is commonly used in recent studies (e.g., [2,3]) to classify a ground motion as the long- or short-duration one. Intensive research efforts have been made to characterize the influence of ground motion duration on structural damage since 1980s, as critically reviewed and summarized by Hancock and Bommer [4] in 2006. They concluded that the influence is dependent to damage measures employed, i.e., duration almost does not affect peak response measures while it does affect cumulative damage measures. It is worth noting that ground motions or loading protocols used in the studies as reviewed by Hancock and Bommer [4] did not well isolate the influence of amplitude and frequency content of ground motions. In this regard, later on some researchers modified spectral contents of recorded short- and long-duration ground motions [5–7] or created stochastically simulated accelerograms [8] to have similar amplitude and frequency contents but different duration properties. To further reserve the characteristics of recorded ground motions that lead to reasonable structural responses as far as possible, Chandramohan et al. [2] set up spectrally matched (in an equivalent level) short- and long-duration record sets with unmodified spectral contents. Owing to the availability of these comparable motion sets as well as the development of experimental and numerical modeling techniques, a number of studies using probabilistic and deterministic analyses are performed on single degree-of-freedom models and building structures (e.g., [9–11], among others), but relatively few on bridges [12]. These studies mostly claimed that duration can influence not only cumulative damage measures such as collapse risk but also peak response measures such as column drift due to the consideration of strength and stiffness deterioration, geometric nonlinearity and P- Δ effect in structural modeling. It should be noted that these studies practically ignored soil-foundation-structure interaction.

Earthquake-induced soil liquefaction and concomitant lateral spreading has been witnessed a serious natural hazard that causes a great deal of damage to bridges in the past few decades [13]. Such damage is often too complex to be well predicted in current structural design practice due to complex soil-foundation-structure interaction, high levels of uncertainties in ground motion characteristics (e.g., amplitude, frequency content, and duration) and variabilities in structural and soil properties. It has been widely recognized the potential for triggering liquefaction and damaging lateral spreading is highly related to the duration properties of motions [14]. However, rare studies examined the effect of ground motion duration on the performance of bridges in liquefied and laterally spreading ground. There is only one directly related study by Khosravifar and Nasr [15], who compared moment-curvature demands of a specific bridge pile-shaft in a specific lateral spreading prone site under one pair of spectrally matched short- and long-duration motions, and reported that inelastic demands are amplified in the long-duration counterpart. Apparently, more studies accounting for the high levels of uncertainties in soil and structural as well as ground motions are required to reduce the gap on this topic, which motivates the current study.

This study aims to identify the influence of duration on seismic fragility of bridges in liquefiable and laterally spreading ground. A coupled soil-pile-bridge finite element (FE) model is built in *OpenSees* [16] considering multiple sources of uncertainties in structural and geotechnical materials, profiles and geometrics. 91 pairs of spectrally equivalent short- and long-duration ground motion records are adopted as seismic input to isolate the influence of amplitude and frequency content.

2. Soil-Bridge Modeling and Ground Motions

2.1 Study object and FE modeling

The study object is a portfolio of multi-span girder bridges with multiple bents individually supported by an extended pile-shaft with fairly uniform distribution of strength and stiffness. The pile-shafts are embedded into similar gently sloping ground consisting of a clay crust layer overlying a liquefiable loose sand layer and



a dense sand layer that can trigger lateral spreading hazard under earthquakes. In this regard, the study object is simply represented by a single bent, as shown in **Fig.1(a)**.

A coupled soil-pile-bridge FE model is built in *OpenSees* [16], as illustrated in **Fig.1(b)**. Four-node-quad elements with PDMY material are adopted to represent sand, while PIMY material is used for the clay crust. In light of Wang et al. [17], a soft interlayer element with a lower value of reference shear modulus $G_{r,soft} = 85 \text{ kPa}$ and a thickness $h_w = 0.5 \text{ m}$ is built to mimic the shear localization phenomenon that is often observed between the liquefied loose sand layer and the clay crust in gently sloping ground [18]. Reinforced concrete pile-shafts are represented by displacement-based beam-column elements with fiber sections shown in **Fig.1(b)**. Concrete and rebars are simulated using Concrete04 (**Fig.1(c)**) and Steel02 models (**Fig.1(d)**), respectively. Soil-pile-interaction is modeled using zero-length elements with PySimple1 (horizontal) and TzSimple1 (vertical) materials for the clay crust while PyLiq1 and TzLiq1 materials for the sand layers, which account for the influence of liquefaction. QzSimple1 material is used for the vertical resistance at the pile tip. The deck is represented by a lumped mass and linked to the top of the extended pile-shaft through a zero-length element with bilinear force-deformation relationship to simulate commonly used elastic rubber bearings [19] (**Fig.1(e)**). It should be noted that this simplified soil-structure coupled modeling technique has been validated by the authors [17,20] using three different centrifuge tests in literature and has been applied in several former studies [21,22].

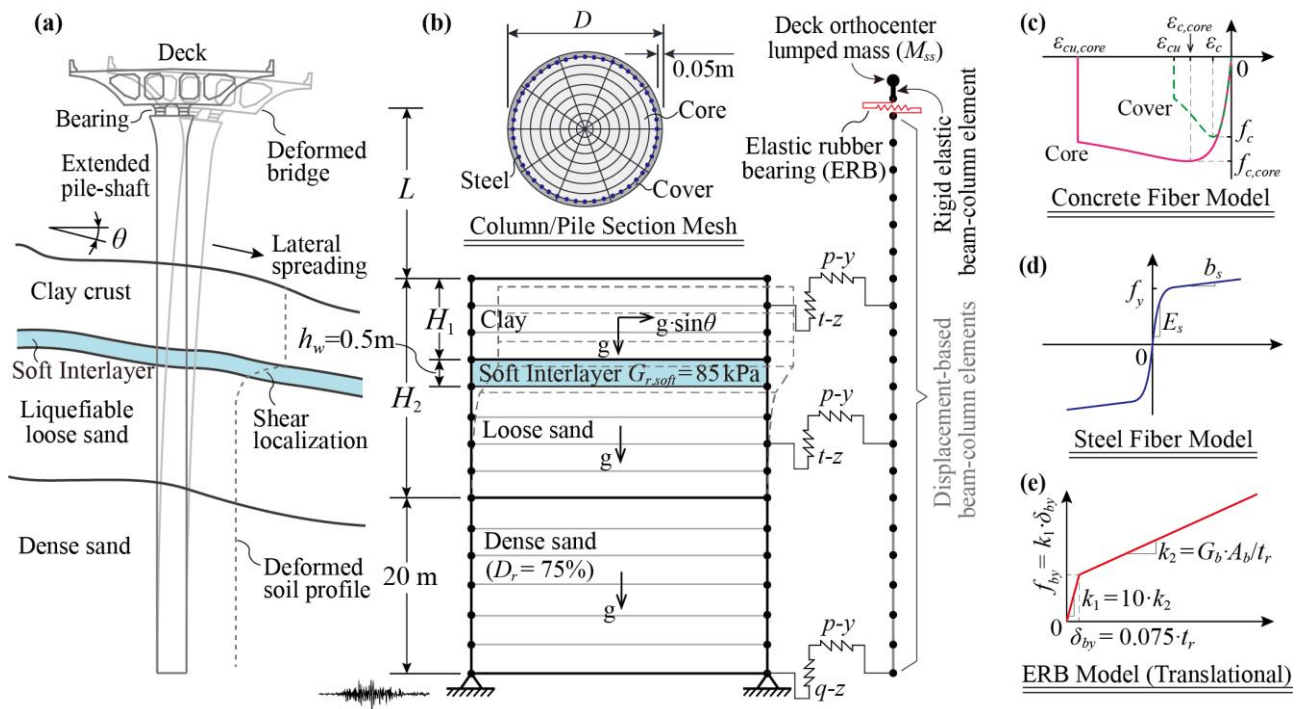


Fig.1 – Schematic illustration of soil-bridge finite element modeling

2.2 Modeling uncertainty consideration

Multiple sources of uncertainties including structural and geotechnical materials, profiles and geometrics are considered in the above-described FE models (**Fig.1**). **Table 1** lists the considered 16 parameters and their descriptions, distribution models and associated means and coefficients of variance (COV) as well as the sources of references. It should be noted that due to the lack of solid evidence, the angle of gently sloping ground is assumed to follow a uniform distribution with lower and upper boundaries of 0 and 8 degrees, respectively.

Latin hypercube sampling is applied to randomly create 91 cases and randomly paired to the selected 91 ground motion records as described later.



Table 1 – Uncertainty consideration of structural and geotechnical parameters

Category	Parameter (Unit)	Description	Distribution	Mean	COV (%)	Reference
Structural	f_c (MPa)	Concrete cover compressive strength	Lognormal	34	18	[23]
	ε_c (/)	Concrete cover strain at the strength	Lognormal	0.002	20	[24]
	ε_{cu} (/)	Concrete cover ultimate strain	Lognormal	0.005	20	[24]
	f_y (MPa)	Rebar yield strength	Lognormal	400	5	[25]
	E_s (GPa)	Rebar elastic modulus	Lognormal	200	3.3	[24]
	b_s (/)	Rebar post-yield hardening ratio	Lognormal	0.01	20	[24]
	D (m)	Column diameter	Normal	2	10	[20]
	L (m)	Column height	Normal	6.5	26	[26]
	α	Column axial load ratio	Normal	0.06	12	[26]
	ρ_l (%)	Longitudinal reinforcement ratio	Normal	1.5	27	[26]
	ρ_s (%)	Transverse reinforcement ratio	Normal	0.5	42	[26]
Geotechnical	S_u (kPa)	Clay undrained shear strength	Lognormal	55	32	[27]
	D_r (%)	Liquefiable sand relative density	Normal	37	19	[27]
	H_1 (m)	Depth at bottom of clay layer	Lognormal	3.1	56	[28]
	H_2 (m)	Depth at bottom of liquefiable layer	Lognormal	5.2	30	[28]
	θ (Degree)	Ground slope angle	Uniform	0 [†]	8 [‡]	/

[†] Lower boundary for uniform distribution;
[‡] Upper boundary for uniform distribution.

2.3 Adopted long- and short-duration ground motion records

Ninety one (91) pairs of spectrally equivalent short- and long-duration accelerograms from Chandramohan et al. [2] are adopted in this study as input at the bottom of the soil. **Fig.2** compares their acceleration spectra and associated mean and 16th/84th percentile. Apparently, they are well matched across periods of interest (0 ~ 6 s), indicating equivalent amplitude and frequency content but different duration.

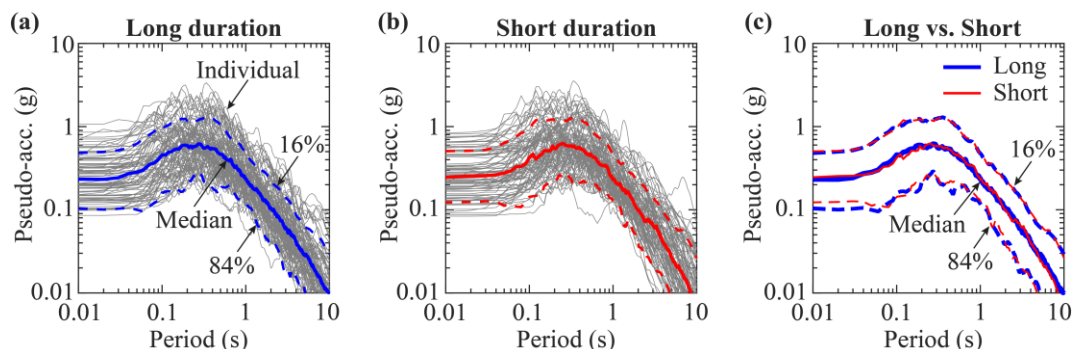


Fig.2 – Acceleration spectra and their median and dispersion (16th and 84th percentile) characteristics of adopted spectrally equivalent (a) long-, (b) short-duration motion sets, and (c) their comparison

Moreover, **Fig.3** depicts an example of short- and long-duration accelerograms recorded during 2008 Wenchuan and 2004 Niigata earthquakes, respectively. Comparisons of acceleration spectra in ordinary and lognormal spaces (**Figs.3(b)** and **(c)**) verify their equivalence in both amplitude and frequency content.

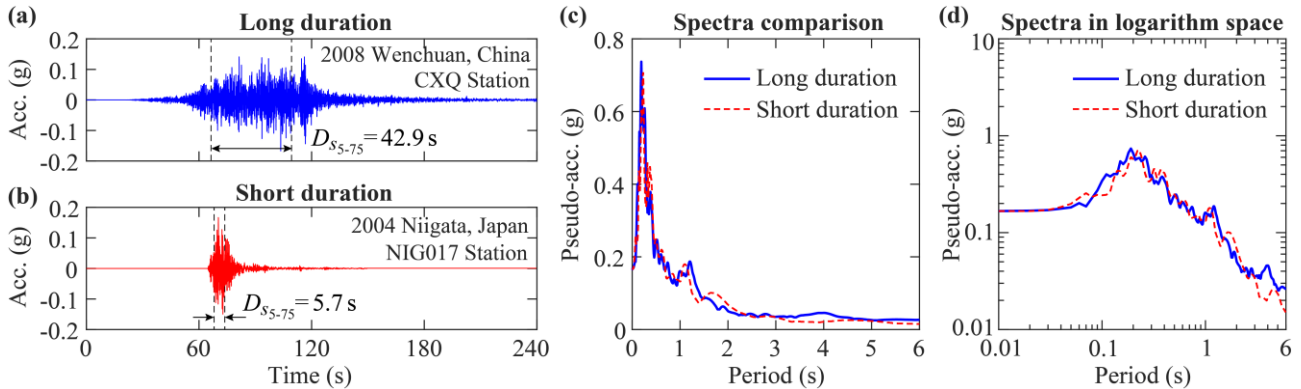


Fig.3 – An example of spectrally equivalent short- and long-duration ground motion pair: (a) long-, (b) short-duration motion time histories, and their acceleration spectra in (c) ordinary and (d) logarithm spaces

Furthermore, **Fig.4** compares intensity measure (IM) properties of the short- and long-duration motion sets. The assessed IMs include peak ground acceleration (PGA), peak ground velocity (PGV), modified cumulative absolute velocity (CAV₅) [29], Housner spectrum intensity (HI) [30], and spectral acceleration at 2.0 s (S_{a20}). These IMs, except for PGA, were found to be correlated well with seismic demands of bridges in liquefied and laterally spreading ground [31]. From Fig.4, it can be seen that the short-duration set generally has slightly larger PGA and PGV values as compared to the long-duration set. By contrast, the long-duration set exhibits dominantly larger CAV₅ value due to its overwhelmingly greater significant duration ($D_{S_{5-75}}$). Since CAV₅ has been proved to be an optimal indicator for soil liquefaction [29], it is reasonable to infer that the long-duration motion set can trigger a higher level of liquefaction. In addition, the other two spectrum-based IMs (HI and S_{a20}) are almost the same between the short- and long-duration sets, as expected.

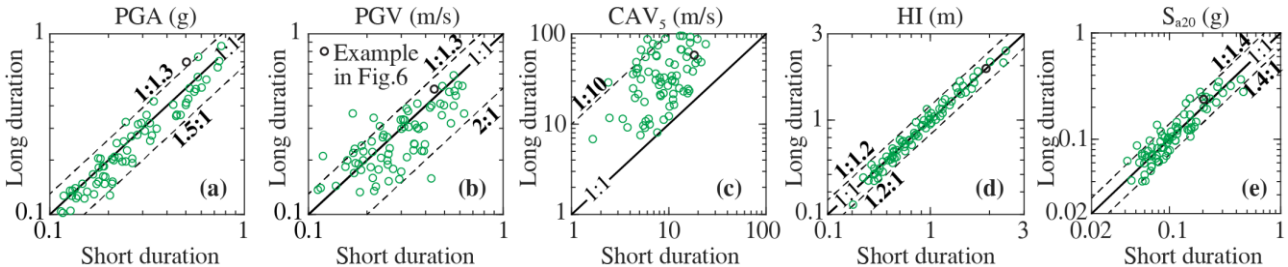


Fig.4 – Comparison of intensity measures of the adopted spectrally equivalent short- and long-duration ground motion sets: (a) PGA, (b) PGV, (c) CAV₅, (d) HI, (e) S_{a20}

3. Typical Results of Dynamic Analyses: Long- versus Short-Duration Motions

To provide an overall insight of the influence of long-duration motions on the seismic demands of bridges in laterally spreading ground, **Fig.5** compares the soil and structural demands between two motion sets. These demand parameters can generally characterize seismic damage to the studied bridges [21]. It is seen that the

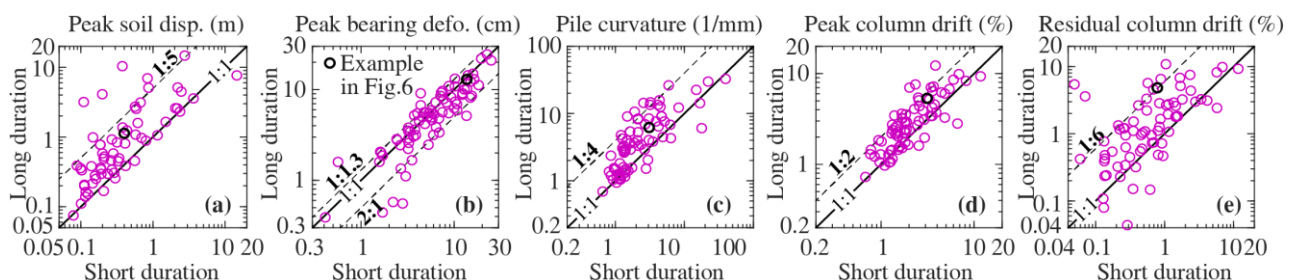


Fig.5 – Comparison of different engineering demand parameters under long- and short-duration motion sets: (a) peak soil lateral spreading displacement, (b) peak bearing deformation, (c) pile-shaft curvature, (d) peak column drift ratio, and (e) residual column drift ratio

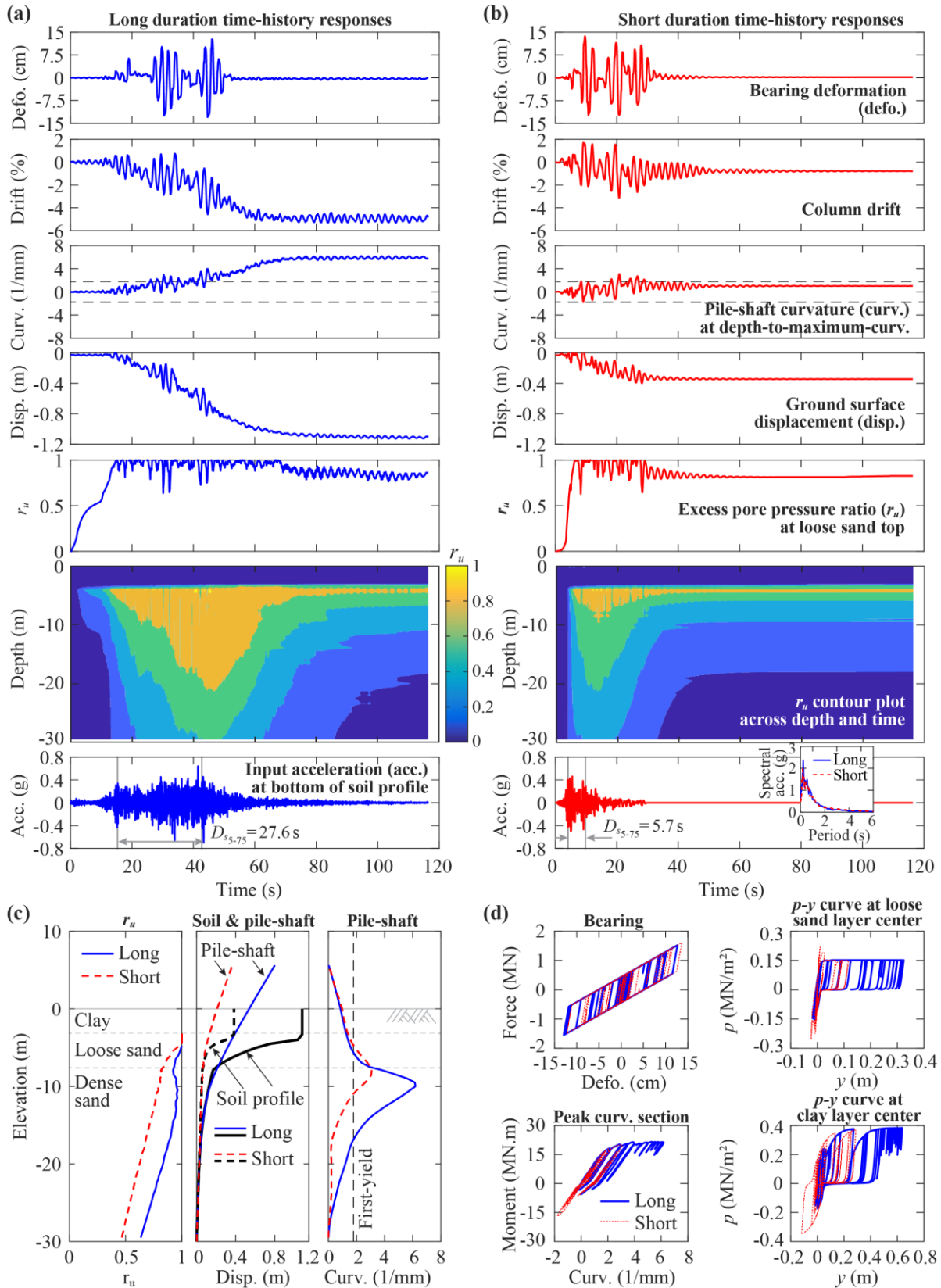


Fig.6 – An example of seismic responses under a pair of long- and short-duration motion sets: time history responses under (a) long- and (b) short-duration motion, (c) envelope distribution, and (d) bearing and soil spring force-displacement responses and section moment-curvature relationship



long-duration set triggers significantly greater lateral spreading displacement, as large as nearly 5 times, as compared to the short-duration counterpart (**Fig.5(a)**), because of the higher level of liquefaction that leads to the larger lateral spreading displacement. Such significant soil displacement demands inevitably impose noted kinematic forces on the pile-shaft. Therefore, seismic demand tendencies under the long-duration set are witnessed as great as nearly 4, 2, and 6 times for pile curvature, peak column drift, and residual column drift, respectively, as compared to those under the short-duration set (**Figs.5(c) to (e)**). However, peak bearing deformation does not show a larger tendency (**Fig.5(b)**); rather it shows a slightly smaller tendency under the long-duration set. This may be partially because the peak bearing deformation is independent on the ground lateral spreading but relevant to PGA of ground motions where the short-duration set contains a bit larger PGA values than the long-duration set as previously shown in **Fig.4(a)**. Overall, long-duration motions tend to amplify the soil lateral spreading displacement, pile curvature and column drift, but have less influence on the bearing deformation.

Fig. 6 depicts an example of seismic responses under a pair of long- and short-duration motion records (1985 Valparaiso and 1994 Northridge earthquakes, respectively). Ground motion and response properties are marked in **Figs.4** and **5** using black circles. From the time history results in **Figs.6(a)** and **(b)**, a higher level of liquefaction (represented by excess pore pressure ratio, r_u) is observed across both excitation time and soil depth under the long-duration set, which consequently leads to larger responses in soil displacement, column drift and pile curvature. However, the bearing deformation demand is quite close even the long-duration motion has a notably greater PGA value (approximately 1.3 times as illustrated in **Fig.4(a)**). This may be attributed to the more severe damage to the pile-shaft under the long-duration motion that elongates the vibration period of the bridge and thereby reduce the seismic load imposed on the bearing. From **Fig.6(c)**, the envelope of r_u response across the depth is obviously aggravated under the long-duration motion, leading to a larger lateral displacement of the clay crust and thereby triggering a greater column deflection and pile curvature nonlinearity. These results can be further observed from **Fig.6(d)** in terms of component force-displacement responses and section moment-curvature relationship at the depth-to-maximum-curvature.

4. Fragility Assessment: Long- versus Short-Duration Motions

4.1 Fragility analysis methodology

Fragility analysis is a critical component for performance-based risk assessment [32], which describes the conditional probability that the demand (D) of a structure meet or exceed its capacity (C) at a specific level of damage state under a given ground motion IM, as commonly expressed by:

$$P[D \geq C | IM] = 1 - \Phi \left(\frac{\ln(S_C) - \ln(S_D)}{\sqrt{\beta_C^2 + \beta_D^2}} \right) \quad (1)$$

where $\Phi(\bullet)$ is the standard normal cumulative distribution function, S_D and S_C are median values of the demand and capacity, respectively, β_D and β_C are logarithmic standard deviations of the demand and capacity, respectively. The demand can be estimated by probabilistic seismic demand model using Cloud method [33]:

$$S_D = a \cdot IM^b \quad (2)$$

where a and b are regression parameters. The dispersion of the demand model can be estimated by Eq.(3).

$$\beta_{D|IM} = \sqrt{\frac{\sum_{i=1}^N [\ln(d_i) - \ln(S_D)]^2}{N - 2}} \quad (3)$$

where d_i is the i th realization of the demands obtained from the time history analyses and N is the number of the analyses ($N=91$ in this study). It is acknowledged that the selection of IM can significantly affect the accuracy of demand estimate and therefore an optimal IM is paramount for fragility analysis. In this study, S_{a20} is adopted based on the authors' former study [31] as well as the fact that the short- and long-duration motion sets have equivalent S_{a20} values (**Fig.4(e)**).



The capacity estimates (i.e., limit states) indicate the level at which structural components resist the demands exerted on the bridge. Based on expert judgment and experimental observations in literature, **Table 2** lists threshold median values and their logarithmic dispersions of four limit states (i.e., slight, moderate, severe, and complete) for the studied engineering demand parameters, including peak bearing deformation, pile curvature, and peak and residual column drifts.

Table 2 – Median (S_c) and logarithmic dispersion (β_c) properties of considered four damage limit states

EDP (Unit)	Slight		Moderate		Severe		Complete		Reference
	S_c	β_c	S_c	β_c	S_c	β_c	S_c	β_c	
Peak bearing defo. (cm)	7.50	0.79	11.25	0.68	15	0.73	18.75	0.66	[19,34]
Pile curvature (1/mm)	1.88	0.11	16.07	0.26	31.16	0.32	44.96	0.33	†
Peak column drift (%)	1.45	0.10	2.60	0.20	4.30	0.29	6.90	0.29	[35]
Residual column drift (%)	0.25	0.25	0.75	0.25	1.00	0.46	1.50	0.46	[36]

† Derived from section moment-curvature analyses considering structural uncertainties. The slight state refers to rebar first-yielding, the moderate state means concrete cover crushing, the severe state represents strain at concrete core reaches two thirds of its crushing strain, and the complete state indicates the core crushing.

4.2 Fragility results and discussion

Based on the fragility analysis methodology described above, fragility curves can be derived. **Fig.7** compares structural fragility under the long- and short-duration motion sets in terms of different engineering demand parameters at different limit states. From **Fig.7(a)**, the long-duration motion set leads to larger probability of exceedance for peak bearing deformation as compared to the short-duration counterpart across all four limit states. This result follows the above finding that the bearing deformation demands tend to be lower under long-duration ground motions. This result also indicates that bridges designed under short-duration ground motions generally leads to conservative results under spectrally matched long-duration ground motions. As for pile curvature, column peak and residual drifts, apparently larger damage probabilities are observed at all studied limit states, implying that the long-duration motions generally bring adverse effects and should be considered in the seismic design of bridge.

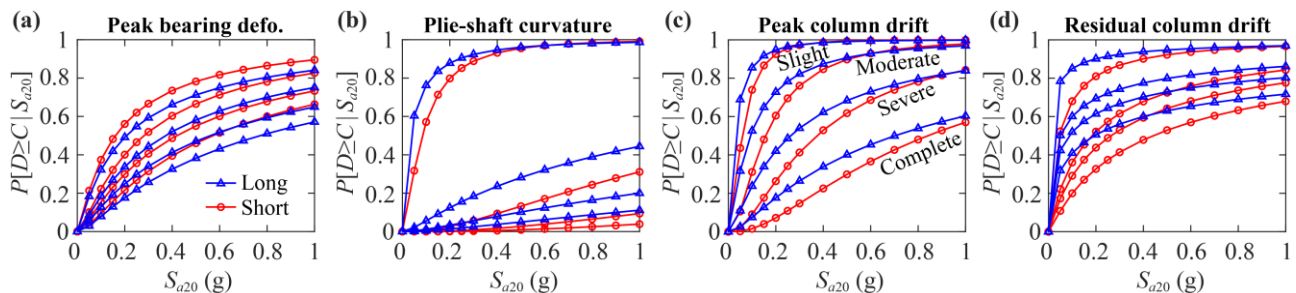


Fig.7 – Comparison of fragility curves under long- and short-duration motions for different bridge components: (a) peak bearing deformation, (b) pile-shaft curvature, (c) peak column drift ratio, and (d) residual column drift ratio

5. Conclusions

This paper identifies the influence of ground motion duration on seismic demands and fragility of extended pile-shaft-supported bridges in liquefied and laterally spreading ground leveraging spectrally matched short- and long-duration ground motion records. Various geotechnical and structural demand parameters, including soil displacement, peak bearing deformation, pile curvature, and peak and residual column drifts, under the short- and long-duration motion sets are compared to reach the following main conclusions.



- 1) Long-duration ground motions significantly aggravate the level of liquefaction across both time and soil depth, leading to significant amplitudes of soil lateral spreading displacement as great as approximately 5 times to that under short-duration ground motions.
- 2) Regarding peak bearing deformation, bridges designed under short-duration ground motions generally leads to conservative results under spectrally matched long-duration counterparts. Thus, for convenience, the effect of duration can be ignored for estimates of bearing deformation.
- 3) For pile curvature and column drift, long-duration motions generally bring adverse effects to amplitude the demands as large as 2~6 times to short-duration motions. Such influence should be considered in the seismic design of bridges for these demand parameters.

6. Acknowledgements

This work is partially supported the China Postdoctoral Science Foundation (Grant Nos. 2018M640448 and 2019T120380). The second author acknowledges the funding provided by the Gulf Research Program of the US National Academies of Sciences, Engineering, and Medicine (Grant No. 2000010987) and US Department of Defense Navy Office of Naval Research (Grant No. N00014-20-1-2055). The third author thanks to the funding provided by the Natural Science Foundation of China (Grant No. 51778469).

7. Copyrights

17WCEE-IAEE 2020 reserves the copyright for the published proceedings. Authors will have the right to use content of the published paper in part or in full for their own work. Authors who use previously published data and illustrations must acknowledge the source in the figure captions.

8. References

- [1] Hancock J, Bommer JJ. The effective number of cycles of earthquake ground motion. *Earthq Eng Struct Dyn* 2005;34:637–64. doi:10.1002/eqe.437.
- [2] Chandramohan R, Baker JW, Deierlein GG. Quantifying the influence of ground motion duration on structural collapse capacity using spectrally equivalent records. *Earthq Spectra* 2016;32:927–50. doi:10.1193/122813EQS298MR2.
- [3] Barbosa AR, Ribeiro FLA, Neves LAC. Influence of earthquake ground-motion duration on damage estimation: application to steel moment resisting frames. *Earthq Eng Struct Dyn* 2017;46:27–49. doi:10.1002/eqe.2769.
- [4] Hancock J, Bommer JJ. A state-of-knowledge review of the influence of strong-motion duration on structural damage. *Earthq Spectra* 2006;22:827–45. doi:10.1193/1.2220576.
- [5] Hancock J, Bommer JJ. Using spectral matched records to explore the influence of strong-motion duration on inelastic structural response. *Soil Dyn Earthq Eng* 2007;27:291–9. doi:10.1016/j.soildyn.2006.09.004.
- [6] Montejo LA, Kowalsky MJ. Estimation of frequency-dependent strong motion duration via wavelets and its influence on nonlinear seismic response. *Comput Civ Infrastruct Eng* 2008;23:253–64. doi:10.1111/j.1467-8667.2007.00534.x.
- [7] Ou Y-C, Song J, Wang P-H, Adidharma L, Chang K-C, Lee GC. Ground motion duration effects on hysteretic behavior of reinforced concrete bridge columns. *J Struct Eng* 2014;140:04013065. doi:10.1061/(ASCE)ST.1943-541X.0000856.



- [8] Sideras SS, Kramer SL. Potential implications of long duration ground motions on the response of liquefiable soil deposits. 9th Int. Conf. Urban Earthq. Eng. / 4th Asia Conf. Earthq. Eng., Tokyo, Japan: 2012.
- [9] Raghunandan M, Liel AB. Effect of ground motion duration on earthquake-induced structural collapse. *Struct Saf* 2013;41:119–33. doi:10.1016/j.strusafe.2012.12.002.
- [10] Barbosa AR, Ribeiro FLA, Neves LAC. Influence of earthquake ground-motion duration on damage estimation: application to steel moment resisting frames. *Earthq Eng Struct Dyn* 2017;46:27–49. doi:10.1002/eqe.2769.
- [11] Hou H, Qu B. Duration effect of spectrally matched ground motions on seismic demands of elastic perfectly plastic SDOFS. *Eng Struct* 2015;90:48–60. doi:10.1016/j.engstruct.2015.02.013.
- [12] Kabir MR, Billah AHMM, Alam MS. Seismic fragility assessment of a multi-span RC bridge in Bangladesh considering near-fault, far-field and long duration ground motions. *Structures* 2019;19:333–48. doi:10.1016/j.istruc.2019.01.021.
- [13] Cubrinovski M, Haskell J, Winkley A, Robinson K, Wotherspoon L. Performance of bridges in liquefied deposits during the 2010–2011 Christchurch, New Zealand, earthquakes. *J Perform Constr Facil* 2014;28:24–39. doi:10.1061/(ASCE)CF.1943-5509.0000402.
- [14] Kramer SL, Greenfield MW. Effects of long-duration motions on soil liquefaction hazards. 16th World Conf. Earthq. Eng., IAEE; 2017.
- [15] Khosravifar A, Nasr J. Modified design procedures for bridge pile foundations subjected to liquefaction-induced lateral spreading. *DFI J - Deep Found Inst* 2017;11:114–27. doi:10.1080/19375247.2018.1436382.
- [16] McKenna F, Scott MH, Fenves GL. Nonlinear finite-element analysis software architecture using object composition. *J Comput Civ Eng* 2010;24:95–107. doi:10.1061/(ASCE)CP.1943-5487.0000002.
- [17] Wang X, Luo F, Su Z, Ye A. Efficient finite-element model for seismic response estimation of piles and soils in liquefied and laterally spreading ground considering shear localization. *Int J Geomech* 2017;17:06016039. doi:10.1061/(ASCE)GM.1943-5622.0000835.
- [18] Kamai R, Boulanger R. Characterizing localization processes during liquefaction using inverse analyses of instrumentation arrays. In: Hatzor YH, Sulem J, Vardoulakis I, editors. *Meso-Scale Shear Phys. Earthq. Landslide Mech.*, London: CRC Press; 2009, p. 219–38. doi:10.1201/b10826-23.
- [19] Zhang J, Huo Y. Evaluating effectiveness and optimum design of isolation devices for highway bridges using the fragility function method. *Eng Struct* 2009;31:1648–60. doi:10.1016/j.engstruct.2009.02.017.
- [20] Wang X, Ye A, Ji B. Fragility-based sensitivity analysis on the seismic performance of pile-group-supported bridges in liquefiable ground undergoing scour potentials. *Eng Struct* 2019;198:109427. doi:10.1016/j.engstruct.2019.109427.
- [21] Wang X, Shafieezadeh A, Ye A. Optimal EDPs for post-earthquake damage assessment of extended pile-shaft-supported bridges subjected to transverse spreading. *Earthq Spectra* 2019;35:1367–96. doi:10.1193/090417EQS171M.
- [22] Wang X, Ye A, Shafieezadeh A, Padgett JE. Fractional order optimal intensity measures for probabilistic seismic demand modeling of extended pile-shaft-supported bridges in liquefiable and laterally spreading ground. *Soil Dyn Earthq Eng* 2019;120:301–15. doi:10.1016/j.soildyn.2019.02.012.
- [23] Pang Y, Wu X, Shen G, Yuan W. Seismic fragility analysis of cable-stayed bridges considering different sources of uncertainties. *J Bridg Eng* 2014;19:04013015. doi:10.1061/(ASCE)BE.1943-5592.0000565.
- [24] Barbato M, Gu Q, Conte JP. Probabilistic push-over analysis of structural and soil-structure systems. *J Struct Eng* 2010;136:1330–41. doi:10.1061/(ASCE)ST.1943-541X.0000231.



- [25] Celarec D, Dolšek M. The impact of modelling uncertainties on the seismic performance assessment of reinforced concrete frame buildings. *Eng Struct* 2013;52:340–54. doi:10.1016/j.engstruct.2013.02.036.
- [26] Brandenberg SJ, Kashighandi P, Zhang J, Huo Y, Zhao M. Fragility Functions for Bridges in Liquefaction-Induced Lateral Spreads. *Earthq Spectra* 2011;27:683–717. doi:10.1193/1.3610248.
- [27] Jones A, Kramer S, Arduino P. Estimation of uncertainty in geotechnical properties for performance-based earthquake engineering. Berkeley, CA: Pacific Earthquake Engineering Research Center; 2002.
- [28] Wang X, et al. Working title: Influence of ground motion duration on resilience quantification of bridges in liquefied and laterally spreading ground leveraging spectrally equivalent motion sets. In-Preparation-for-Submission 2020.
- [29] Kramer SL, Mitchell RA. Ground motion intensity measures for liquefaction hazard evaluation. *Earthq Spectra* 2006;22:413–38. doi:10.1193/1.2194970.
- [30] Housner GW. Spectrum intensities of strong motion earthquakes. *Proceedings, Symp. Earthq. Blast Eff. Struct.*, 1952, p. 21–36.
- [31] Wang X, Shafieezadeh A, Ye A. Optimal intensity measures for probabilistic seismic demand modeling of extended pile-shaft-supported bridges in liquefied and laterally spreading ground. *Bull Earthq Eng* 2018;16:229–57. doi:10.1007/s10518-017-0199-2.
- [32] Padgett JE, DesRoches R. Methodology for the development of analytical fragility curves for retrofitted bridges. *Earthq Eng Struct Dyn* 2008;37:1157–74. doi:10.1002/eqe.801.
- [33] Cornell CA, Jalayer F, Hamburger RO, Foutch DA. Probabilistic basis for 2000 SAC federal emergency management agency steel moment frame guidelines. *J Struct Eng* 2002;128:526–33. doi:10.1061/(ASCE)0733-9445(2002)128:4(526).
- [34] Nielson BG, Desroches R. Seismic fragility methodology for highway bridges using a component level approach. *Earthq Eng Struct Dyn* 2007;36:823–39. doi:10.1002/eqe.
- [35] Li J, Spencer BF, Elnashai AS. Bayesian updating of fragility functions using hybrid simulation. *J Struct Eng* 2013;139:1160–71. doi:10.1061/(ASCE)ST.1943-541X.0000685.
- [36] Muntasir Billah AHM, Shahria Alam M. Seismic fragility assessment of concrete bridge pier reinforced with superelastic shape memory alloy. *Earthq Spectra* 2015;31:1515–41. doi:10.1193/112512EQS337M.